

ESFuelCell2012-91008

HIGH DENSITY THERMAL ENERGY STORAGE WITH SUPERCRITICAL FLUIDS

Gani B. Ganapathi

Jet Propulsion Laboratory, California Institute of
Technology
Pasadena, CA, USA

Richard Wirz

University of California Los Angeles
Los Angeles, CA, USA

ABSTRACT

A novel approach to storing thermal energy with supercritical fluids is being investigated, which if successful, promises to transform the way thermal energy is captured and utilized. The use of supercritical fluids allows cost-affordable high-density storage with a combination of latent heat and sensible heat in the two-phase as well as the supercritical state. This technology will enhance penetration of several thermal power generation applications and high temperature water for commercial use if the overall cost of the technology can be demonstrated to be lower than the current state-of-the-art molten salt using sodium nitrate and potassium nitrate eutectic mixtures. An additional attraction is that the volumetric storage density of a supercritical fluid can be higher than a two-tank molten salt system due to the high compressibilities in the supercritical state.

This looks at different elements for determining the feasibility of this storage concept - thermodynamics of supercritical state with a specific example, naphthalene, fluid and system cost and a representative storage design. A modular storage vessel design based on a shell and heat exchanger concept allows the cost to be minimized as there is no need for a separate pump for transferring fluid from one tank to another as in the molten salt system. Since the heat exchangers are internal to the tank, other advantages such as lower parasitic heat loss, easy fabrication can be achieved.

Results from the study indicate that the fluid cost can be reduced by a factor of ten or even twenty depending on the fluid and thermodynamic optimization of loading factor. Results for naphthalene operating between 290 °C and 475 °C, indicate that the fluid cost is approximately \$3/kWh compared with \$25-\$50/kWh for molten salt. When the storage container costs are factored in, the overall system cost is still very attractive. Studies for a 12-hr storage indicate that for operating at temperatures between 290-450 °C, the cost for a molten salt system can vary between \$66/kWh to \$184/kWh depending on molten salt cost of \$2/kg or a more recent quote of \$8/kg. In

contrast, the cost for a 12-hr supercritical storage system can be as low as \$40/kWh. By using less expensive materials than SS 316L, it is possible to reduce the costs even further.

INTRODUCTION

Solar thermal power (also called “Concentrated Solar Thermal” (CST)) is viewed as the most cost-effective option to convert solar radiation into electricity, and has been operationally proven in California since the mid-1980s. In 1984, the first SEGS (solar electric generating systems) plant was installed in southern California by Luz International, Inc. The most recently commissioned plant was in 2008, a 64MW plant, Nevada Solar One and purchase agreements for nearly 1 GW of solar thermal have been completed, or are in the final stages, in the southwest U.S.

One advantage of parabolic trough power plants is their potential for storing solar thermal energy to use during non-solar periods and to dispatch when it's needed most. As a result, thermal energy storage (TES) allows parabolic trough power plants to achieve higher annual capacity factors—from 25% without thermal storage up to 70% or more with it. The other related advantages include the capability of buffering during transient weather conditions, improved dispatchability or time-shifting, more even distribution of electricity production and capability to achieve full load operation of the steam cycle at high efficiency.

The Department Of Energy (DOE) has identified improved thermal energy storage (TES) as the most critical technology development needed to allow solar thermal power to replace non-renewable power generation sources (i.e. coal, gas). The DOE estimates that the cost of TES has to be around \$20/kWh⁽¹⁾ to make a significant impact on power production with CSP by bringing the cost down from current 11-13 ¢/kWh to ~ 7 ¢/kWh by 2015 with 6 hours of storage for intermediate power markets and to ~ 5 ¢/kWh by 2020 with 16 hours of storage for baseload power markets. The currently favored thermal storage option is 2-stage indirect storage with molten salts (eutectic

mixtures of NaNO_3 and KNO_3) for which the fluid costs alone range from \$25 - \$50/kWh. Clearly a breakthrough is needed to meet the DOE cost goal of \$20/kWh. This proposal presents an alternate approach to providing thermal energy storage which promises to meet the DOE cost goals.

Thermal energy storage systems are broadly rated on the following technical requirements⁽²⁾

1. High energy density of the storage material (per-unit mass or per-unit volume)
2. Good heat transfer between heat transfer fluid (HTF) and the storage medium
3. Mechanical and chemical stability of storage material
4. Chemical compatibility between HTF, heat exchanger and/or storage medium
5. Complete reversibility for a large number of charging/discharging cycles
6. Low thermal losses
7. Ease of control

In terms of cost, the following factors are important - cost of the storage material itself, heat exchanger for charging and discharging the system and the cost for the space and the enclosure for the TES.

The 3 mechanisms for storage can be broadly classified as under sensible heat storage, latent heat storage and chemical storage. The different storage systems that have been studied include⁽³⁾:

1. *Two-tank direct* where the heat transfer fluid (HTF) is also used as the storage fluid. It was first demonstrated in the Luz trough plant, SEGS and operated between 1985 and 1999 to dispatch solar power to meet SCE winter evening peak demand period needs.
2. *Two-tank indirect* where term indirect refers to the fact that the storage fluid is different from the HTF. The heat from the HTF is transferred to one of the tanks which is then transferred to the power generation system when needed by discharging the fluid into another tank through the use of heat exchangers. Molten salt eutectic mixtures of KNO_3 and NaNO_3 are used for the storage medium. This system is currently favored over the other options even though the costs of the storage fluid are very high, due to its maturity. The most advanced implementation of its type is the Andasol 1 plant in Spain (shown schematically in Figure 1) with a storage capacity of 1 GWh (7.5 hr full load operation).
3. *Single Tank Thermocline*. In this system, one tank stores both the hot fluid as well as the cold fluid by taking advantage of the fact that a hot fluid is lighter than cold and will remain at the top. Sandia National Laboratories has demonstrated a 2.5 MWh packed-bed thermocline system with molten salt fluid and quartzite rock and sand for filler material.
4. *Thermal Energy Storage Media*. Solid TES media such as concrete, castable ceramic materials are being considered as potential TES candidates. This is primarily driven by the low cost of the solid media itself as well as other advantages such as long life. The HTF passes through an

array of pipes embedded in the solid medium to transfer the thermal energy to and from the medium during plant operations. The German Aerospace Center (DLR) and Ciemat have performed initial testing of castable ceramic and high-temperature concrete.

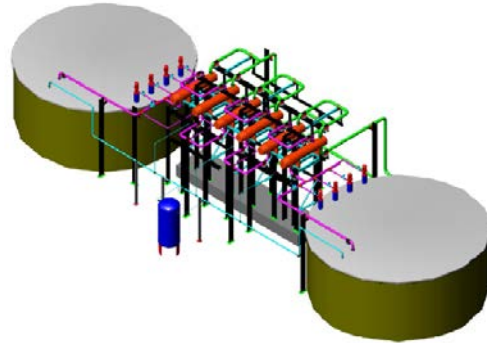


Figure 1 Two-tank indirect storage (Andasol-1; 1 GWh storage).

All the technologies mentioned above rely on sensible heat. Phase change materials (PCMs) in contrast rely on the latent heat and can therefore store large amounts of heat. The DOE had studied the possibility of using PCM in the 80's for heat storage, but didn't pursue it further primarily due to 1) complexities of the system, 2) uncertainty over lifetime of the PCMs. Work performed by Luz International Ltd. on use of low temperature salts such as NaNO_3 , KNO_3 , and KOH indicated that the performance of the materials degrade after a moderate number of freeze-melt cycles. Additionally, the heat transfer characteristics for PCMs have two major problems 1) relatively poor thermal conductance across regions of solid PCM compared to convective heat transfer in the heat transfer fluid (HTF) and 2) pinch-point problem which refers to the relatively small temperature differences between the PCM and the charging or discharging HTF which occurs in the heat exchanger where the PCM is just dropping below or rising above the phase change temperature. At these points, due to the small temperature differences, large heat transfer areas are needed for the transfer of heat.

More recently, the DOE has reinitiated funding for TES and HTF and has funded several proposals to the tune of \$68M in 2008⁽⁴⁾, to look at alternate technologies as well as address many of the problems with prior approaches. For the most part the technologies proposed were either sensible heat-based approaches or very advanced technologies, where it is not clear that will solve the fundamental problem – i.e., low-cost storage. Discussions with NREL indicated a breakthrough approach is needed to solve the cost goal of \$20/kWh. In the following section, an alternate approach will be presented which promises to meet the cost goal while simultaneously solving many of the issues faced by the current baseline approach of 2-tank molten salt storage.

SUPERCRITICAL STORAGE

This concept relies on latent heat storage as in the case of PCM but works with a liquid instead. The approach is based on a few fundamental thermodynamic concepts:

1. By using the latent heat of liquid/vapor phase change, it is possible to develop an efficient system which will provide a constant sink/source of heat, and
2. By operating the TES system at a higher pressure, it is possible to increase the saturation temperature and thus operate at molten salt temperatures and above.
3. By storing heat at supercritical conditions and removing heat while crossing over the two-phase regime, significant amount of heat stored in latent form can be extracted with relatively moderate penalty for volume expansion due to the high compressibility in supercritical state.

This concept can be better visualized with a phase diagram as shown in Figure 2⁽⁵⁾.

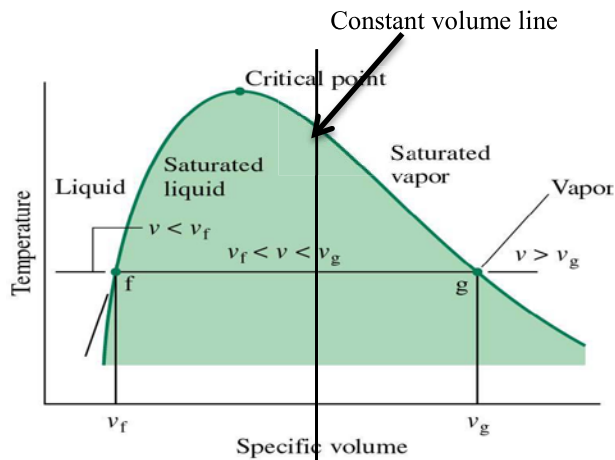


Figure 2 Phase diagram for a pure component.

The “tie-line” fg represents the two-phase regime. By adding heat into the liquid at f, the enthalpy of the liquid/vapor system increases till it is all vapor at g. During this phase change in an enclosed system as more heat is introduced, the pressure (and temperature) of the system increases till a new equilibrium point is reached as one goes up on the constant volume line. It is then possible to design a system where the entire fluid is in a supercritical state (above and right of critical point). In such a state it is possible to optimize the volume of the overall system to be more compact due to the high compressibility in that state. Of course, the price to pay is a higher system pressure. However, with a judicious choice of working fluid the system pressure needn't be excessive. In a sense, this concept is meant to operate similar to steam accumulators which are used in chemical process plants to provide short duration thermal energy storage primarily for buffering variations in heat production. However, there are some key differences – storage with this concept is done with a fixed amount of fluid that doesn't change and heat transfer within the storage medium is done entirely in the fluid media

through internal heat exchangers. The advantages of this will be discussed later.

The selection of fluid is crucial to the working of the TES. An initial effort was focused towards organic fluids. The selection of fluids is based on the following criteria:

1. High heat of vaporization, $\Delta_{\text{vap}}H$
2. High critical temperature, T_c , and boiling point, T_b

Fluids that can provide significant heat storage temperatures close to molten salt at 657K (384°C) were targeted for initial selection. Four hundred organic fluids⁽⁶⁾ were rapidly reviewed for the right mix of thermodynamic properties identified above. A down select of approximately ten liquids were made with an initial preference for ones with a good combination of thermodynamic properties, material compatibilities and cost. Thermodynamic properties were estimated using approaches outlined in Reid, et al⁽⁶⁾. For candidate fluids, the estimation was cross-checked with data in the literature at discrete temperature values.

Thermodynamic properties for a select few fluids are shown in Table 1 based on the estimation approaches recommended by Reid, et al⁽⁶⁾.

Table 1 Thermodynamic properties for initial down selected TES candidates

Fluid Name	T_c (K)	T_b (K)	ΔH_{vap} (J/kg)	ΔH_{vap} (J/kg) (@ 657K)
Pthalic Anhydride	810	560	334736	270134
Benzoic acid	752	523	414549	282167
Naphthalene	748	491	337530	219760
3,4 Xylenol	729	500	401121	244072
Glycerol	726	563	663298	439789
Iodobenzene	721	461	193602	109946

A quick analysis was performed using the approach provided by Reid et al.⁽⁶⁾. A more detailed approach is used in the system model.

SELECTION OF FLUID

Four hundred organic fluids were rapidly reviewed for the right mix of thermodynamic properties. The downselect was initially done for utility scale operating temperatures (>384 °C). Initial screening indicated glycerol as being an ideal candidate based both on performance and cost. Also, there was a projected glut in the market projected due to its being formed as a byproduct in the process of making biofuels. However, initial testing with this fluid found it to be thermally unstable at temperatures approaching critical temperatures, and the next best fluid in terms of fluid cost and feasibility was identified as being naphthalene. Testing with this fluid both at JPL in 2010 and in UCLA in 2011 indicated the feasibility of using naphthalene.

On-going studies at UCLA is proceeding to identify other fluids.

Initial performance trades for a few fluids including supercritical glycerol and naphthalene are shown in Table 2.

Even though naphthalene prices are higher than bulk glycerol prices, it is clear that as a supercritical fluid, it far outperforms the current state-of-the-art molten salt system.

However, it is important to note that these are only fluid costs. To truly evaluate costs at the system level, it is important to determine the impact of operating at the higher pressures on tank storage material costs.

Table 2. Comparison of storage fluid costs at sub-critical and supercritical states

Moderate Temperature Application ($T_{\text{cold}} = 373\text{K}$, $\Delta T = 100\text{K}$)			
	Specific Storage (kJ/kg)	Volumetric Storage Capacity (kJ/m ³) (vapor press at 200 °C)	\$/kWh (\$/kg)
Compressed water	418	362,000 (15 atm)	Negligible
Therminol (VP-1)	229	228,700 (<1 atm)	78 (\$/kg)
Glycerol	241	303,850 (<1 atm)	8 (\$0.55/kg)
Naphthalene	200	216,609 (<1 atm)	16 (\$1/kg)
High Temperature Application ($T_{\text{cold}} = 563\text{K}$, $\Delta T = 100\text{K}$)			
Supercritical Glycerol	720	324,741 (66 atm, $z = 0.25$)	2.75 (\$0.55/kg)
Supercritical Naphthalene	541	387,122 (66 atm, $z = 0.219$)	6.50 (\$1.00/kg)
Molten Salt (NaNO ₃ , KNO ₃)	145	129,860 (2 tanks)	25 – 50 (\$1-\$2/kg)

The results from the fluids study was quite clear on the superiority of using supercritical fluids for storing thermal energy.

SYSTEM COST

The next task was to determine the overall system costs based on loading a fixed volume storage container and determining the change in the system enthalpy as the temperature is changed from one state to another. For this a detailed thermodynamic model for naphthalene was developed using the three parameter Peng-Robinson equation of state (P-R EOS). The three parameters used in the EOS are (P_c , T_c , ω) where P_c , is the critical pressure, T_c is the critical temperature, and ω is the Pitzer's acentric factor. The P-R EOS is expressed as

$$P = \frac{RT}{V-b} - \frac{a}{V^2 + 2Vb - b^2} \quad (1)$$

where a and b are given by

$$a = \frac{0.457236R^2\alpha T_c}{P_c}$$

and where

$$\alpha = \left(1 + (0.37464 + 1.5422\omega - 0.26992\omega^2) \left\{ 1 - \sqrt{\frac{T}{T_c}} \right\} \right)^2$$

The choice of the P-R EOS was settled upon after comparing hand calculated results from Lee-Kestler (L-K), a more accurate model, and P-R EOS to some known values from literature. While the L-K was indeed more accurate, the difference was less than 6% compared to literature values, but the implementation was a lot harder. The initial effort focused on determining optimal fill conditions and end pressure, temperatures using material costs (fluid and storage container) as the objective function to minimize.

MODELING APPROACH

Departure functions are suitable for determining changes in state properties such as enthalpy, internal energy, etc. The enthalpy departure function can be derived from the Helmholtz departure function. For constant temperature and composition, the departure function for Helmholtz energy is given by

$$A - A^0 = \int_{V^0}^V \left(P - \frac{RT}{V} \right) dV + RT \ln \frac{V}{V^0} \quad (2)$$

and the entropy departure function

$$S - S^0 = \frac{\partial}{\partial T} (A - A^0) = \int_{V^0}^V \left[\left(\frac{\partial P}{\partial V} \right)_T - \frac{R}{V} \right] dV + R \ln \frac{V}{V^0} \quad (3)$$

Since the enthalpy departure, $H - H^0$, is given by

$$H - H^0 = (A - A^0) + T(S - S^0) + RT(Z - 1) \quad (4)$$

Then,

$$H - H^0 = RT_c \left[T_r(Z - 1) - 2.078(1 + \kappa) \sqrt{\alpha} \ln \left(\frac{Z + 2.414B}{Z - 2.414B} \right) \right] \quad (5)$$

where, $T_r = T/T_c$, $P_r = P/P_c$, $\kappa = 0.37464 + 1.5422\omega - 0.26992\omega^2$, $B = 0.07780P_r/T_r$, and ω is the Pitzer acentric factor.

If a fluid at T_1 , P_1 is taken to a new state T_2 , P_2 , then the change in enthalpy, ΔH between the two states can be expressed as

$$H[T_2, P_2] - H[T_1, P_1] = (H[T_2, P_2] - H^0[T_2, P_0]) + (H^0[T_2, P_0] - H^0[T_1, P_0]) + (H^0[T_1, P_0] - H^0[T_1, P_1]) \quad (6)$$

where the first terms in brackets correspond to enthalpy departure for state 2, the second terms in brackets correspond to ideal gas enthalpy change between state 1 and 2, and the last term terms in bracket correspond to the negative departure function for state 1. The ideal gas enthalpy change can be calculated from

$$H^0[T_2, P_2] - H^0[T_1, P_0] = \int_{T_1}^{T_2} C_p^0(T) dT \quad (7)$$

where $C_p^0(T)$ is the heat capacity of naphthalene ideal gas. The reference pressure choice is arbitrary, though for enthalpy calculations, $P=0$ is used.

CALCULATIONS AND RESULTS

The three parameters used in the P-R EOS for naphthalene are $P_c = 4.068$ MPa (590 psia), $T_c = 478.4$ °C and $\omega = 0.309$.

The calculations were done for a fixed volume of 1 m^3 and the loading (percentage of volume at 25 °C) was the key variable. Four cases for final pressures at 4.2 MPa (609 psia), 6.895 MPa (1000 psia), 10.342 MPa (1500 psia) and 13.789 MPa (2000 psia) were selected as the final (charged state) pressure, and the initial temperature was fixed at 290 °C, representing the typical discharge temperature in a two-tank

storage system, where the hot tank is at 390 °C and the cold tank is at 290 °C.

At the initial temperature, the naphthalene is in a two-state (liquid and vapor) condition, and P_1 is equal to the vapor pressure of naphthalene at T_1 .

From the initial loading condition and molar volumes of the vapor and liquid obtained from the P-R EOS, the quality of the fluid at initial state can be calculated. For the final state, there are two unknowns, T_2 and Z_2 . The two equations needed to solve for both are the P-R EOS and the $PV=znRT$.

A sample result for the case where the final pressure is $P_2 = 6.895$ MPa (1000 psia) is shown in Figure 3.

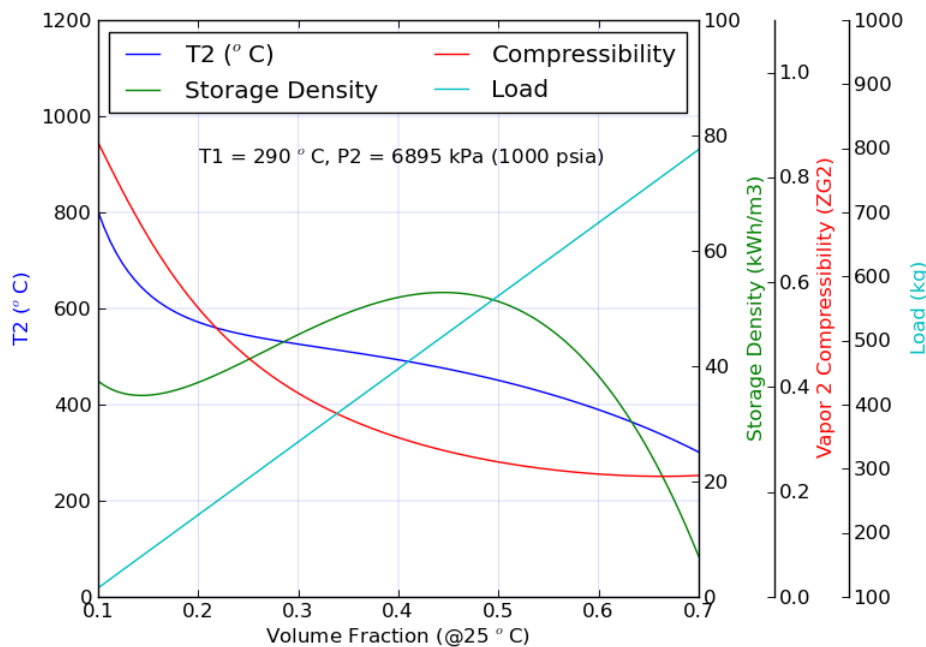


Figure 3. Storage density vs volume fraction

The results in the figure need some explanation. The x-axis represents the volume fraction of naphthalene (solid at 25°C) and the y-axis is the final temperature when the final pressure, P_2 , is fixed at 6.895 MPa. The cyan line is the weight of naphthalene loaded initially at the different volume fractions. The red line is the vapor compressibility, the blue line is the final temperature and the green line is the energy density. When the initial loading is very low, say 10% of total volume, it would take a final temperature of ~ 900 °C to reach the final pressure of 6.895 MPa. The final state is almost an ideal gas with a compressibility of above 0.9. When the loading is increased, the final state compressibility keeps decreasing and the storage density goes through a peak, which is close to the critical point incidentally in this case. The peaking in storage

density is because as the loading fraction increases, latent heat plays a larger role in the storage. However, when the load increases beyond a certain point, the liquid volume is so high that the final pressure is reached and not much heat is absorbed. When the calculations were done for all the cases, it was seen

that there is a trade-off between working at higher pressures or temperatures. The calculations were repeated for the other end

state pressures and similar peaks in the storage densities were obtained.

In the next stage, a costing analysis incorporating the cost of materials (fluid and storage container) were used to calculate the optimal operating point.

For the analysis, stainless steel TP316 was selected because of its known corrosion resistance to a wide variety of fluids. Commercial vendor data was used to determine the nominal tube wall thickness for different nominal tube O.D. The data

used in the study was nominal pressure ratings for seamless or welded and drawn, fully annealed stainless steel tubing conforming to ASTM A213, ASTM A249 or ASTM 269 respectively. These pressure ratings were derived from the Lamé formula with 130MPa (18,800 psi) allowable stress and approximately 4:1 design factor. For derating the steel at higher temperatures, a value of 0.6 was used for temperatures between 400 °C and 500 °C. As seen in Figure 4 a derating of 0.6 is a

conservative value for allowable stress for TP316H.

Seamless Austenitic Alloys Steel Pipes

Operating temperature and allowable stresses in pipe walls for seamless austenitic alloys steel pipes A-312 and A-369

- grade TP304H, TP321H, TP347H, TP348H and TP316H

are indicated in the diagram below:

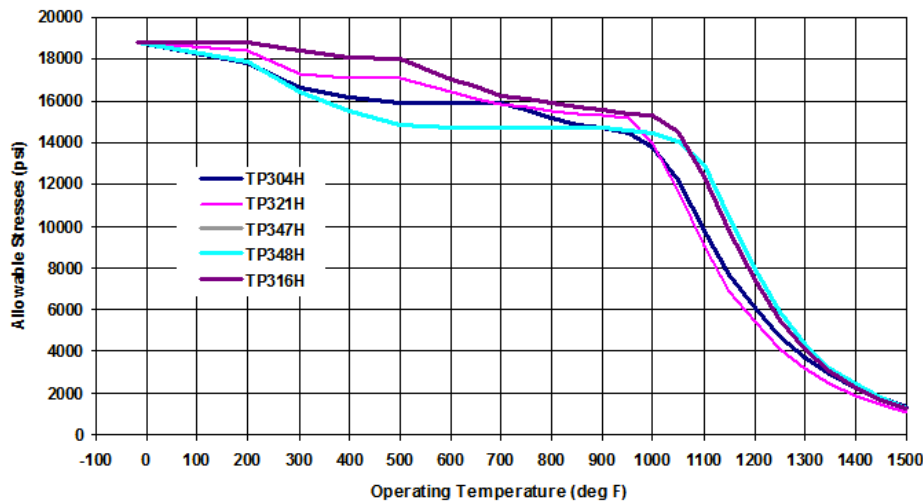


Figure 4. Allowable stress for seamless austenitic alloys steel pipes (ref: http://www.engineeringtoolbox.com/temperature-allowable-stresses-pipes-d_1338.html)

Thus, as an example, for operating at 1000 psia, 500 °C, tubing with a rating of 1666 psia at room temperature is needed, which would dictate a tube of thickness $\geq 0.0093''$. Based on internet search, it was possible to find pricing of SS 316H and in bulk the rates on alibaba.com were $\sim \$1.40/\text{kg}$. Similarly, the price of naphthalene was around $\$0.36/\text{kg}$. For the costing analysis, the same set of conditions were imposed as for the thermodynamics-alone analysis. The constraint on the problem was to not let T_2 exceed 500 °C as the allowable stress drops precipitously as seen in Figure 4. For all cases, 2" OD tubing was chosen, with the exception of the 2000 psia case, where no tubing available beyond 1.75" OD were available. The analysis included the thermal capacity of the steel as well as the fluid and results for the case where $P_2 = 1000$ psia, is shown in Figure 5. For this particular case, where the final pressure was fixed at 1000 psia, and the final temperature was not allowed to exceed 500 °C, the optimum storage density of 84.8 kWh/m^3 was obtained for an initial loading of $\sim 439 \text{ kg/m}^3$. The results from this case and the others are shown below in Table 3.

The results in Table 3 indicate that though the storage density increases as the final pressure is allowed to go higher, the penalty is a higher total cost as the cost of metal starts making a big difference. The table also includes the cost $\$/\text{kWh}$ for molten salt assuming $\$2/\text{kg}$. The cost of just the salt alone is $\$29.30/\text{kWh}$ which compares with $\$2.17/\text{kWh}$ for supercritical fluid alone. However, while the cost of the storage tank for the molten salt is not shown here, it is expected to be lower than the storage cost for supercritical fluid.

Following this study a full analysis comparing the cost of using molten salt and supercritical fluids was conducted for an utility-scale with 6-, 12- and 18-hour storage capacity. A 100 MW_e utility plant was used from a report by Worley Parsons ⁽⁷⁾. For the study, naphthalene was again used as the candidate supercritical fluid with a bulk cost of $\$0.33/\text{kg}$. Molten salt cost was assumed to be $\$2/\text{kg}$, but the study also looked at the case where molten salt was quoted at $\$8/\text{kg}$. Another assumption for the supercritical tank was that when manufactured in large quantities, only the material cost will dominate. The supercritical storage tank was assumed to have internal heat

exchangers as it was based on a shell-and-tube heat exchanger design with heat transfer fluid flowing over the storage fluid inside tubes. The results from this study are shown Table 4.

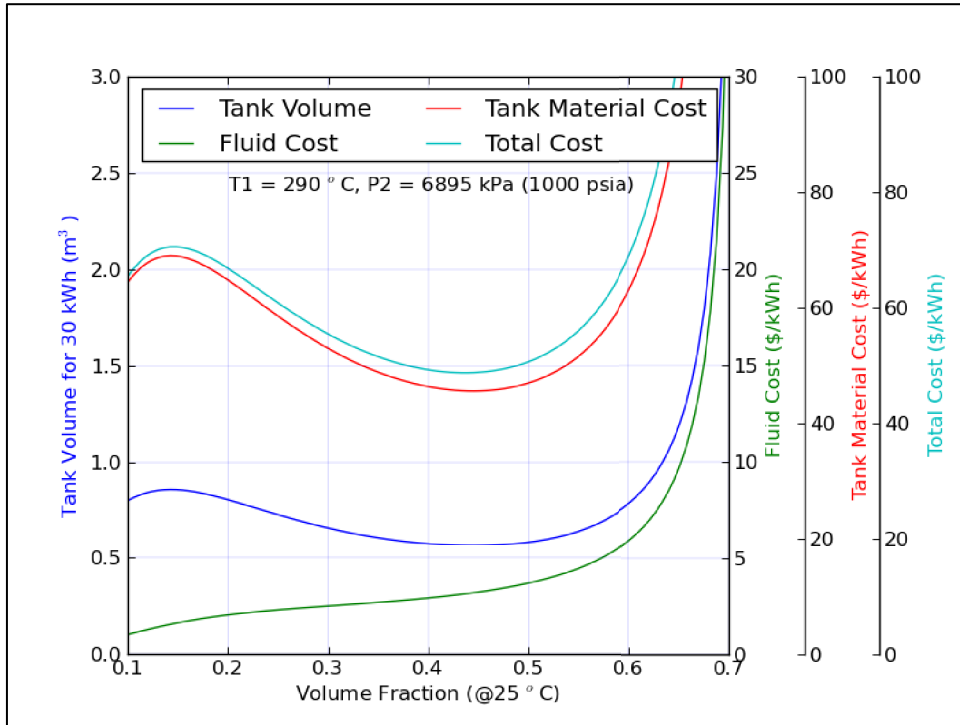


Figure 5. System cost trades for naphthalene ($P_2 = 1000$ psia).

There results from Table 4 are quite illuminating. It shows that even when the salt cost is assumed to be \$2/kg, the total cost for a 6-hr storage is \$59/kWh while the cost for supercritical fluid storage system is \$39/kWh. The study has ignored the cost of molten salt tank costs and the shell cost for the supercritical storage system since they are equivalent in costs. In order to understand why the total cost is lower than a molten salt system, one needs to look at all the equipment needed for a molten salt system which is not needed for a supercritical fluid storage system. In particular, the two major cost drivers are the

dedicated pump and heat exchanger for the molten salt system which are not needed for the supercritical fluid system. When the true of current molten salt is taken into account, the total cost goes up quite dramatically from \$59/kWh to \$246/kWh.

Table 3. Summary of optimal costs at different end states

P_2 (psia)	T_2 (°C)	Storage Density (kWh/m ³)	Load (kg/m ³)	Fluid Cost (\$/kWh _t)	Tank Cost (\$/kWh _t)	Total Cost (\$/kWh _t)	Salt Cost (\$/kWh _t) (@\$2/kg)
609	461	70.0	460	2.17	23.02	25.19	29.30
1000	498	84.8	439	1.71	28.43	30.14	24.91
1500	492	99.4	535.5	1.78	37.52	39.3	22.19
2000	499.6	112	570	1.68	44.88	46.57	22.18

Table 4 . Cost comparison between supercritical and molten salt

	6-hr storage	12-hr storage	18-hr storage	Notes
Net Power (MW _e)	103	103	103	Ref.
Gross Power (MW _e)	118	118	118	
Rankine effc.	37.4%	37.4%	37.4%	
Thermal storage (MWh _t)	1893	3786	5679	
Temp range (500-375 °C) for supercritical fluid	125	125	125	
Temp range (500-390 °C) for molten salt	110	110	110	Assumes same bypass ops.
Molten Salt (HiTec Solar Salt) T ₁ = 500 °C/T ₂ = 390 °C				
Cp salt (J/kg/K)	1550	1550	1550	
Mass Salt (10 ⁶ kg)	52	104	156	includes 30% stagnant excess
Cost of salt (\$M) (@ \$2/kg)	104	208	312	
Cost of salt (\$M) (@\$8.80/kg)	457	915	1372	
Pumps+HEX (\$M)	30	45	60	No pump, Hex in single tank
Tanks (\$M)	43	64.5	86	Tank cost removed
Piping, Insulation, Valves, Fittings (\$M)	1.5	1.5	1.5	
Foundation & Support Structures (\$M)	0.5	0.75	1	x1.5 factor
Instrumentation & Control (\$M)	6	6	6	
Total \$M (@\$2/kg)	112	216	320	Tank cost removed
Total \$M (@\$8.80/kg)	465	923	1380	Tank cost removed
Salt \$/kWh _t (@ \$2/kg)	55	55	55	
Total \$/kWh _t (@ \$2/kg)	59	57	56	
Salt \$/kWh _t (@\$8.80/kg)	242	242	242	
Total \$/kWh _t (@8.80/kg)	246	244	243	
Supercritical Fluid (Naphthalene @ T ₁ =500°C/T ₂ =375°C, 880 psia)				
Fluid Cost (\$/kWh _t)	2	2	2	Naphthalene (\$0.33/kg bulk)
Tank material cost (\$/kWh _t)	33	33	33	SS 316L (\$1.40/kg bulk)
Total Fluid cost (\$M)	3.8	7.6	11.4	
Tank Material cost (\$M)	62	125	187	
Pumps + HEX (\$M)	0.0	0.0	0.0	Internal HEX single tank
Piping, Insulation, Valves, Fittings (\$M)	1.5	1.5	1.5	same as for salt
Foundation & Support Structures (\$M)	0.5	0.75	1	same as for salt
Instrumentation & Control (\$M)	6	6	6	same as for salt
Total \$M	74	141	207	
Total \$/kWh _t	39	37	36	

Company. The authors also want to thank their team members for helping out on this project.

SUMMARY AND CONCLUSIONS

This paper presents a novel approach using supercritical fluids to store thermal energy with a much higher storage density than the state of the art, two-tank molten salt. In addition, the cost of the chosen fluid is much lower than molten

salt and the difference will continue to grow as the demand for nitrates grow for use as fertilizer. A robust program to develop alternate fluids is being studied at UCLA and a prototype storage tank is in the process of being developed for testing at JPL. Results from the testing will be used for building larger-sized tanks as the processes get worked out.

ACKNOWLEDGEMENTS

Part of this research was carried out at the Jet Propulsion Laboratory, California Institute of Technology, under a contract with the National Aeronautics and Space Administration. This effort was supported by ARPA-E Award DE-AR0000140 and Grant No. 5660021607 from the Southern California Gas

REFERENCES

1. *2008 Solar Annual Review Meeting*. Greg Glatzmaier, Mark Mehos, Tom Mancini. s.l. : NREL & SNL, 2008.
2. *Overview on Thermal Energy Storage for Trough Power Systems*. Ulf Hermann, Michael Geyer (FLABEG Solar Int. GmbH), Dave Kearney (Kearney & Assoc). Feb 20-21, 2002.
3. http://www.nrel.gov/csp/troughnet/thermal_energy_storage.html. NREL.
4. <http://www.energy.gov/news/6562.htm>. DOE. 2008.
5. Mark Zemansky, Michael Abbott, Hendrick Van Ness. *Basic Engineering Thermodynamics*. s.l. : McGraw Hill, 1975.
6. Robert Reid, John Prausnitz, Thomas Sherwood. *The Properties of Gases and Liquids*. s.l. : McGraw Hill, 1977. 3rd Ed.
7. *CSP Parabolic Trough Plant Cost Assessment*, WorleyParsons Group, Report under NREL contract KAXL-9-99205-01